

Manuscript Number: RADMEAS-D-14-00423R3

Title: Low temperature thermochronology using thermoluminescence signals from quartz

Article Type: SI: LED2014

Keywords: Thermochronology; Luminescence; ITL; TL; Quartz; protocols

Corresponding Author: Dr. Sheng-Hua Li,

Corresponding Author's Institution: The University of Hong Kong

First Author: Shuang-Li Tang

Order of Authors: Shuang-Li Tang; Sheng-Hua Li

Abstract: Isothermal thermoluminescence (ITL) and thermoluminescence (TL) signals from quartz were studied. A single aliquot regenerative dose protocol has been applied for ITL D_e determination (SAR-ITL). In the SAR-ITL protocol, the preheat condition was a cutheat to 10 °C higher than measurement temperature. The test dose was approximate to the expected D_e , and a 450 °C heat was given at end of each cycle to minimize signal build-up. Based on signals strength and dose recovery test, temperatures of 235 and 255 °C were selected for the ITL D_e measurement. A multiple aliquots regenerative protocol has been applied for TL D_e determination (MAR-TL). The preheat procedure was a cutheat of 235 °C and a second glow TL of 175 Gy was used for normalization. The sensitivity change of first heating to 450 °C was negligible, supported by comparison between additive and regenerative dose growth curves. Based on the natural TL signal and preheat condition studies, D_e values at temperatures of 250-330 °C were used for thermochronological study. These two protocols were applied to rock samples collected at different elevations from Nujiang River (also called Salween River) valley slope. The SAR-ITL gave D_e results consistent with the MAR-TL at temperatures of 40-50°C higher. The results clearly demonstrate the differences in the thermal histories between the analyzed samples. The SAR-ITL and MAR-TL protocols were both found to be suitable for application in thermochronology.

Abstract

Isothermal thermoluminescence (ITL) and thermoluminescence (TL) signals from quartz were studied. A single aliquot regenerative dose protocol has been applied for ITL D_e determination (SAR-ITL). In the SAR-ITL protocol, the preheat condition was a cutheat to 10 °C higher than measurement temperature. The test dose was approximate to the expected D_e , and a 450 °C heat was given at end of each cycle to minimize signal build-up. Based on signals strength and dose recovery test, temperatures of 235 and 255 °C were selected for the ITL D_e measurement. A multiple aliquots regenerative protocol has been applied for TL D_e determination (MAR-TL). The preheat procedure was a cutheat of 235 °C and a second glow TL of 175 Gy was used for normalization. The sensitivity change of first heating to 450 °C was negligible, supported by comparison between additive and regenerative dose growth curves. Based on the natural TL signal and preheat condition studies, D_e values at temperatures of 250-330 °C were used for thermochronological study. These two protocols were applied to rock samples collected at different elevations from Nujiang River (also called Salween River) valley slope. The SAR-ITL gave D_e results consistent with the MAR-TL at temperatures of 40-50°C higher. The results clearly demonstrate the differences in the thermal histories between the analyzed samples. The SAR-ITL and MAR-TL protocols were both found to be suitable for application in thermochronology.

Key words: Thermochronology; Luminescence; ITL; TL; Quartz; Protocol

1. Introduction

Luminescence dating has been developed as a useful archaeological and geological dating tool since the 1960s (Aitken et al., 1964). For burnt materials like pottery, burnt flint, burnt stone and volcanic lava, thermoluminescence (TL) dating is typically applied. For sedimentary materials like loess, beach dunes, colluvial deposits, fluvial and lacustrine sands, optically stimulated luminescence (OSL) dating is applied. For these materials, the luminescence clock is set to zero before being buried or preserved. Many dating protocols have been established, such as multiple aliquot additive dose thermoluminescence (MAA-TL) protocol (Aitken, 1985), multiple aliquot regenerative dose thermoluminescence (MAR-TL) protocol (Aitken, 1985), single aliquot regenerative dose optically stimulated luminescence (SAR-OSL) protocol (Murray and Wintle, 2000a, 2003; Li et al., 2002; Li and Li, 2011) and single aliquot regenerative dose isothermal thermoluminescence (SAR-ITL) protocol (Jain et al., 2005; Tribolo and Mercier, 2012).

The thermoluminescence signal is temperature sensitive by definition (Johnson, 1966). It has been used as a low temperature thermochronological method for non-burnt rock samples that have experienced cooling processes of exhumation. The fundamental principles, theoretical formulas and numerical simulation have been studied over last 20 years (e.g. Prokein and Wagner, 1994; Herman et al., 2010; Li and Li, 2012). The luminescence dating has a lower closure temperatures and suitable for an age dating range within 1 Myr (Dodson, 1973). With these features, the

1 luminescence could be a very powerful tool to research the low temperature zone
2
3 beyond the established thermochronological techniques, e.g. $^{40}\text{Ar}/^{39}\text{Ar}$, fission tracks
4
5 and (U-Th)/He methods. It can therefore be used to determine the instantaneous
6
7 reaction response to abrupt and rapid crust uplift, such as river incision, glacial
8
9 denudation and normal faulting. In contrast, most of the established
10
11 thermochronological techniques, such as $^{40}\text{Ar}/^{39}\text{Ar}$, fission track and (U-Th)/He dating
12
13 can only measure the average rate of regional exhumation in the order of tens of Myr,
14
15 which is much slower than the true uplift rate of the crust.
16
17
18
19
20
21
22
23
24

25 Numerous previous studies of rock samples have indicated that luminescence signals
26
27 are dependent on thermal history (Nambu et al., 1996; Han et al., 1997; Tsuchiya et
28
29 al., 2000; Herman et al., 2010; Li and Li, 2012). Different from ambient temperature
30
31 condition, the equivalent dose of a cooling system can be expressed as
32
33
34

$$\frac{dD_e}{dt} = D_r - \frac{D_0 \cdot s}{e^{E/KT}} (e^{\frac{D_e}{D_0}} - 1)$$

35 where D_e is the equivalent dose (Gy), D_0 (Gy) is the
36
37 characteristic dose of saturation, D_r (Gy/ka) is the dose rate of radiation, temperature
38
39

40 T (K) is a function of time t (ka), E (eV) is the activation energy of the traps of interest,
41
42 s is the frequency factor described the attempt to escape frequency in second^{-1} , and
43
44 k is the Boltzmann constant (Li and Li, 2012). The quotients that D_e divided by annual
45
46 dose were considered as apparent ages, because D_e is a function of T , t and D_r . For a
47
48 luminescence signal to be used to investigate rock thermal history, the following
49
50 work has to be carried out. 1) Identifying a bright enough luminescence signal. 2)
51
52 Finding an appropriate protocol for D_e measurement. 3) Studying rock
53
54
55
56
57
58
59
60
61
62
63
64
65

1 microdosimetry for the annual dose estimation. 4) Obtaining the D_e values and
2
3 apparent ages that correspond to the closure temperatures. 5) Deriving a cooling
4
5 rate based on the determined trap parameters (E , s and kinetic orders).
6
7
8
9

10
11 In this paper, we aim to investigate suitable protocols through fundamental and
12
13 systematical experimental study. SAR-ITL and MAR-TL protocols were studied for
14
15 thermochronology of rocks.
16
17
18
19
20
21

22 **2. Samples and equipment**

23
24 Three rock samples were collected from a “V” shape valley slope of the Nujiang River
25
26 (Salween River), and named from top to bottom as FG-A, FG-B and FG-C. They are
27
28 mylonite (FG-A), schist (FG-B) and gneiss (FG-C) and contain abundant quartz, and
29
30 have experienced rapid cooling in recent geological history due to the river incision.
31
32
33
34
35
36
37
38

39 The raw samples were sawed using rock cutting machinery and crushed by hand
40
41 hammer gently to maintain the original minerals size. After dry sieving, 150-180 μm
42
43 grain size range was obtained. Quartz grains were separated from bulk mineral grains
44
45 by heavy liquid density separation at 2.62-2.75 $\text{g}\cdot\text{cm}^{-3}$. They were then etched by 40%
46
47 HF for 1 hour to remove the outside layer compromised by alpha particles and
48
49 remaining feldspar grains. All preparations were performed under fluorescent lamp
50
51 or dim red light.
52
53
54
55
56
57
58
59
60
61
62
63
64
65

1 D_e measurements were conducted with a TL/OSL DA15 Risø reader. It is equipped
2
3 with an EMI Q9235 photomultiplier tube with three 2.5 mm Hoya -U340 filters
4
5 attached in front for detection in the UV wavelength range (around 340 nm). A
6
7 ⁹⁰Sr/⁹⁰Y beta source was used for irradiations. The heating rate was 5 °C/s for all
8
9 experiments. The purity of quartz grains was tested by monitoring the presence of
10
11 feldspar through measuring the infrared stimulated luminescence (IRSL) (Duller, 2003)
12
13 and 110 °C thermoluminescence (TL) peak (Li et al., 2002). Unless specified, all the
14
15 ITL and TL experiments used six aliquots of 5 mm diameter for each data point in the
16
17 measurement.
18
19
20
21
22
23
24
25
26
27

28 Three different signals, OSL, ITL and TL, were examined to identify sufficiently bright
29
30 signals. The OSL signal under blue light stimulation (six clusters of LEDs, 470±20 nm)
31
32 was not detected for some rocks. The ITL and TL signals are strong enough in all of
33
34 our rocks samples (Fig. 1).
35
36
37
38
39
40
41

42 **3. SAR-ITL**

43
44 The SAR-ITL signal at 310-330 °C has been used for the dating of sediments in
45
46 previous studies (Choi et al., 2006; Huot et al., 2006). However, in this study lower
47
48 heating temperatures were chosen because they are temperature sensitive and
49
50 correspond to lower thermal stability. These would record the most recent cooling
51
52 processes before the equilibrium state or signal saturation was reached. Sample FG-A
53
54 was used in these experiments.
55
56
57
58
59
60
61
62
63
64
65

1
2
3 The natural TL signal of sample FG-A was detected at temperatures starting from
4
5
6 235 °C. The natural signal of ITL at 235 °C was used for experimentation. The preheat
7
8
9 conditions (Fig. 4A, steps 2 and 5) of the 235 °C ITL signal were varied to identify a
10
11
12 bright enough signal and study the effect on D_e value. Three preheating conditions (a
13
14 preheat for 10s at 235 °C, a cutheat to 235 °C and a cutheat to 245 °C) were
15
16
17 examined for SAR-ITL at 235 °C. The results are displayed in Fig. 2A, B and C. After
18
19 preheat at 235°C for 10s, both the natural and regenerative signal were removed. In
20
21
22 the case of cutheat 235 °C, the first 10s signal of the regenerative dose was much
23
24
25 higher than the natural signal, indicating that the existence of a less stable signal in
26
27
28 the regenerative signals. In the case of a cutheat to 245 °C, the natural and
29
30
31 regenerative signals overlapped each other. The ratio between them was consistent
32
33
34 with ITL heating time except for the first 10s. The ratio between natural and
35
36
37 regenerative signals increases during the first 10s; thermal lag lengthen the time
38
39
40 needed for a disk to reach thermal equilibrium. The cutheat to 235 °C resulted in a
41
42
43 remarkable higher initial signal for the regenerative signals, while the cutheat to
44
45
46 245 °C gave an identical result between natural and regenerative signals. The cutheat
47
48
49 to 10 °C higher was used as the preheating in this study.

50
51
52
53 Different test doses (Fig. 4A, step 4) were studied to evaluate the effect on ITL D_e and
54
55
56 to identify an appropriate test dose value. Three different test doses, 25, 145 and
57
58
59 250 Gy were tested for SAR-ITL at 235 °C on sample FG-A (Fig. 2D). Consistent D_e
60
61
62

1 values of 153.2 ± 25.3 Gy and 147.2 ± 8.1 Gy were obtained by using test doses of
2
3 145 and 250 Gy, respectively. The test dose of 25 Gy gave a D_e value 20 percent
4
5 smaller. This indicates that a test dose of 145 Gy or larger is suitable for sample
6
7 measurement and a test dose approximate to that of the expected D_e should be used
8
9 for the measurement. The D_e values obtained using a test dose of 250 Gy had smaller
10
11 errors than that of 145 Gy. However, it is time consuming on the measurements.
12
13
14
15
16
17
18
19

20 Different thermal wash procedures (Fig. 4A, step 7) were applied at the end of each
21
22 cycle to remove signal build-up. Three different heating temperatures, 0, 350 and
23
24 450 °C were examined to evaluate the effect of signal build-up using sample FG-A (Fig.
25
26 2E). D_e values increase as the thermal wash temperature increases, which is
27
28 attributed to the lower signal build-up as a result of the higher cleaning temperature.
29
30
31 A heating of 450 °C has cleaned the remnant signals thoroughly, according to a
32
33 second TL measurement to 450 °C. This result indicated that a 450 °C cycle heat is
34
35 appropriate.
36
37
38
39
40
41
42
43

44 Different ITL heating temperatures correspond to the thermal chronometers of
45
46 different closure temperatures (except for a single TL peak covering a wide
47
48 temperature range). Five ITL heating temperatures of 215, 235, 255, 275 and 295 °C
49
50 were examined using sample FG-A, where the natural D_e values were estimated using
51
52 SAR-ITL (Fig. 4A, steps 3 and 6). A cutheat to 10 °C higher than ITL temperature was
53
54 used as a preheat. The aliquots were then heated to 500s to obtain the ITL signal.
55
56
57
58
59
60
61
62
63
64
65

1 The first 10-20s and last 50s were integrated as the signal and background
2 respectively. A test dose approximate to the expected D_e was used and a 450 °C heat
3 was applied at the end of each cycle. For dose recovery tests, aliquots were heated
4 for 1 hour at 500 °C, and then were given artificial doses similar to the estimated
5 natural D_e . The measured ratios (measured/given doses) which decrease with ITL
6 heating temperatures, were 0.99 ± 0.09 for 215 °C, 0.97 ± 0.08 for 235 °C, 0.97 ± 0.06
7 for 255 °C, 0.89 ± 0.04 for 275 °C, and 0.88 ± 0.04 for 295 °C. The results in Fig. 3
8 demonstrate that signal intensity increases with temperature, whilst the dose
9 recovery ratio decreases. At 215 °C, although the dose recovery result was excellent,
10 the natural signal was too weak to be measured. For 275 and 295 °C, the ITL signals
11 were bright but the dose recovery tests showed D_e underestimations. Therefore, we
12 used 235 and 255 °C as SAR-ITL measurement temperatures. The recuperation for ITL
13 at 235 and 255 °C was 3.8% and 2.3% respectively and the recycling ratios were 1.10
14 ± 0.11 and 1.04 ± 0.05 respectively. This indicates that the 235 and 255 °C are
15 appropriate as the SAR-ITL measurement temperature.
16
17
18
19
20
21
22
23
24
25
26
27
28
29
30
31
32
33
34
35
36
37
38
39
40
41
42
43
44

45 The measurement conditions of the SAR-ITL protocol were summarized in Fig. 4. Each
46 cycle was composed of the seven steps. A thermal wash (Fig. 4A, step 7) is
47 introduced to ensure no signal build-up after each measurement cycle (Tribolo and
48 Mercier, 2012). The first 10-20s and last 50s are integrated as signal and background,
49 respectively. Unless specified, all the SAR-ITL experiments used six aliquots of 5 mm
50 diameter for each sample in the measurement. SAR-ITL results of three samples were
51
52
53
54
55
56
57
58
59
60
61
62
63
64
65

1 shown in Table 1. For both 235 and 255 °C, the FG-B had the largest D_e (200.6 and
2
3 350.8 Gy), and FG-A had the second largest D_e (153.2 and 258.4 Gy) and FG-C had
4
5 smallest D_e (48.9 and 200.7 Gy). The results demonstrated the differences of the
6
7 thermal histories between samples. Neither positive nor negative correlation can be
8
9 identified between the D_e values and elevations.
10
11
12
13
14
15
16

17 **4. MAR-TL**

18
19 The established SAR-ITL protocol is not perfect, because it is not appropriate for
20
21 measuring temperature over 255°C due to poor recovery dose test. Samples with a
22
23 large D_e would require long measurement periods using the SAR-ITL protocol. To
24
25 obtain multiple signals at different temperatures and to optimize the measurement
26
27 time, the MAR-TL protocol was explored. Sample FG-A was used for the study of
28
29 experimental conditions.
30
31
32
33
34
35
36
37
38

39 An important issue of MAR-TL is whether the regenerative growth curve can
40
41 represent the natural growth curve or not. To verify this, the growth curves of sample
42
43 FG-A were built up using both additive dose and regenerative dose methods. For the
44
45 additive dose method, six groups of six aliquots were given 0, 70, 140, 210, 280 and
46
47 350 Gy respectively. For the regenerative dose method, ten groups of six aliquots
48
49 were given 70, 140, 210, 280, 350, 420, 490, 560, 630 and 700 Gy respectively, after
50
51 an initial resetting at 450 °C. Signals were normalized by the 175 Gy regenerative
52
53 second glows TL. The integrations of TL counts of 5 °C were plotted as a function of
54
55
56
57
58
59
60
61
62
63
64
65

1 given doses in Fig. 5. The regenerative dose growth curve was translated by 250 Gy,
2
3 such that it matched the observed additive dose growth curve (Prescott et al., 1993).
4
5
6 The good similarity in growth curve shape, between additive and regenerated growth
7
8 curves suggest that the thermal resetting did not induce a change in sensitivity in the
9
10 regenerated growth (Mejdahl and Jensen, 1994; Tribolo and Mercier, 2012).
11
12
13
14
15
16

17 The natural TL signal of sample FG-A can be distinguished from backgrounds at
18
19 temperatures higher than 235 °C. Three different cutheat temperatures (Fig. 4B,
20
21 steps 1, 4 and 7), 215, 235 and 255°C were examined in the MAR-TL sequence. The
22
23 D_e values are plotted against temperature using an integration of every 5 °C ($D_e(T)$
24
25 plot) (Fig.6). For each $D_e(T)$ plot, the D_e values at temperature lower than preheat
26
27 temperature are not meaningful. The natural signals were partially or completely
28
29 removed by preheating since these are at lower temperatures. Hence, the
30
31 regenerated doses would dominate these temperature regions. The results in Fig. 6
32
33 indicate that D_e values are higher at TL temperatures 255-300 °C after a cutheat to
34
35 255 °C in comparison with cutheats of 215 and 235 °C. After cutheats of 215 and
36
37 235 °C, the D_e showed the same values with signals from TL temperatures greater
38
39 than 235 °C. For the 300-350 °C, these three curves under different preheat
40
41 conditions overlapped and formed one single curve, indicating that the different
42
43 preheat conditions only has a limited effect on D_e values. Therefore a cutheat to
44
45 235 °C was used as the preheat condition. Still, D_e values of TL below 250 °C can be
46
47 influenced by preheating. Blackbody radiation became significant above 330 °C. The
48
49
50
51
52
53
54
55
56
57
58
59
60
61
62
63
64
65

1 D_e values of TL from 250 to 330 °C were used in thermochronological study. The
2
3 validity of the second glow normalization is evaluated by R-squared value of growth
4
5 fitting (Fig. 4B, step 6). After the normalization, the adjusted R-squared value of
6
7 fitting was 0.9833 in comparing the value of 0.3552 before normalized. Uncertainties
8
9 due to the normalization procedure were included in the total equivalent dose
10
11 uncertainties.
12
13
14
15

16
17
18
19
20 The MAR-TL protocol is summarized in Fig. 4B and the MAR-TL results are shown in
21
22 Table 1. D_e values from 250 to 330 °C at increments of 10 °C are listed. Each D_e is
23
24 calculated from 10°C integration on the lowest 5 and highest 5 degrees. Similar to
25
26 the results of SAR-ITL, no systematic dependence of D_e is found on elevation. For the
27
28 250-330 °C, the FG-B had the largest D_e (76.9-530.3 Gy), and the FG-C had second
29
30 largest D_e (63.3-494.8 Gy) and the FG-A had smallest D_e (49.2-475.0 Gy).
31
32
33
34
35
36
37
38

39 **5. Discussions**

40 41 42 *5.1 Advantages vs. disadvantages*

43
44 The SAR-ITL protocol has following advantages. 1) Only a small amount of materials is
45
46 needed for a D_e measurement. 2) An inter aliquot normalization is not required. 3)
47
48 The sensitivity changes which occur during repeated regeneration and measurement
49
50 cycles can be corrected using the ITL induced by a test dose. 4) The ITL heating
51
52 temperature is lower than conventional TL. The influence of the atmosphere of the
53
54 TL oven at high temperature is not critical for ITL (e.g. nitrogen; Aitken, 1985). 5) The
55
56
57
58
59
60
61
62
63
64
65

1 blackbody radiation is lower during an ITL measurement compared to conventional
2
3 TL. 6) The thermal stability and components of ITL signal can be assessed and
4
5 separated by fitting the decay curves with multi-exponential components (Aitken,
6
7 1985; Huot et al., 2006; Tribolo and Mercier, 2012). There are however disadvantages
8
9 when using the SAR-ITL protocol. 1) The ITL signal may artificially build up over
10
11 measurement cycles if the residual signals are not properly reset. 2) A single aliquot
12
13 protocol requires far longer amounts of measurement time compared to multiple
14
15 aliquots. 3) Quartz from some rocks such as limestone and dolomite might have very
16
17 weak ITL signals.
18
19
20
21
22
23
24
25
26
27

28 The MAR-TL has following advantages. 1) Multiple D_e values of different TL peaks can
29
30 be measured in one run, with each TL peak represents a geothermometer. 2)
31
32 Different TL peaks, representing thermal chronometers of different closure
33
34 temperatures, could provide multiple stage information of cooling processes. 3) The
35
36 kinetics parameters of TL signals have been well studied (Chen and Mckeever, 1997;
37
38 Aitken, 1985; Hornyak et al., 1992). 4) A multiple aliquot TL method requires shorter
39
40 machine time. 5) The thermal stability of TL signals can be identified from the
41
42 temperature of TL glow curve (Aitken, 1985). There are however disadvantages. 1)
43
44 The normalization between aliquots typically increase the dispersion in the growth
45
46 curve. 2) A D_e value may be difficult to interpret if extracted from a temperature
47
48 region that contains one or more overlapping TL peaks. 3) The influences of the
49
50 atmosphere of the TL oven at high temperature need to be accounted for (e.g.
51
52
53
54
55
56
57
58
59
60
61
62
63
64
65

1 nitrogen; Aitken, 1985). 4) The blackbody radiation might influence the TL signal at
2
3 high temperature (>400 °C).
4
5
6
7

8 9 *5.2 Sensitivity change of SAR-ITL*

10
11 The sensitivity change during the first heating of the SAR-ITL protocol has been
12 reported to be a problem in the dating of sediment (Buylaert et al., 2006; Huot et al.,
13 2006). Tribolo and Mercier (2012) identified two groups of burnt quartzites which
14 behaved entirely differently in terms of sensitivity change; they used samples with
15 little or no sensitivity change to determine their equivalent doses. In this study, all
16 samples were evaluated by comparing the additive and regenerative dose TL growth
17 curve (Prescott et al., 1993; Mejdahl and Jensen, 1994). Where growth curves
18 overlapped after sliding, this indicated that sensitivity change after the first heating
19 was not an issue for the samples (Fig. 5). For ITL, because the heating temperatures
20 were relatively low, the first heat sensitivity change is less problematic compared to a
21 TL measurement. It is therefore concluded that the SAR-ITL and MAR-TL protocols
22 used in this study have negligible effects of sensitivity changes (Tribolo and Mercier,
23 2012).
24
25
26
27
28
29
30
31
32
33
34
35
36
37
38
39
40
41
42
43
44
45
46
47
48
49

50 *5.3 Comparison between SAR-ITL and MAR-TL*

51
52 The results from the SAR-ITL and MAR-TL protocols should yield the same $D_e(T)$ plots,
53 which correspond to TL peaks as well as a thermal chronometer. The ITL signal of a
54 certain temperature originates from the traps which correspond to TL peaks at higher
55
56
57
58
59
60
61
62
63
64
65

1 temperatures. Murray and Wintle (2000b) have reported the 330 °C ITL signal came
2
3 from 375 °C TL peak. The D_e values of SAR-ITL appear to be shifted compared with
4
5 the $D_e(T)$ plots of MAR-TL. A 40-50 °C translation is needed to overlap the D_e values
6
7 obtained from SAR-ITL and MAR-TL. This is consistent with the fact that an ITL
8
9 measurement probe trapped electrons held at a deeper TL temperature (Murray and
10
11 Wintle, 2000). Though, it doesn't apply to all D_e values. The FG-C SAR-ITL D_e of $48.9 \pm$
12
13 6.9 Gy appears to be lower than the value expected from MAR-TL after 40 °C shift.
14
15 They overlapped well with a 25 °C shift. This temperature differences might be
16
17 sample dependent and dictated by unique character of these quartz samples. Since
18
19 the traps depth energy (E) increases with the measuring temperature, D_e values
20
21 determined under different temperatures are different. Here, no $D_e(T)$ plateau could
22
23 be obtained (Fig.6). A plateau would be present only if the TL glow curve was
24
25 dominated by a single TL peak, within a temperature range.
26
27
28
29
30
31
32
33
34
35
36
37
38

39 **6. Conclusion**

40
41 The SAR-ITL and MAR-TL protocols were studied and applied to rock samples
42
43 collected from the Nujiang River valley slope. For SAR-ITL, the preheat procedure had
44
45 a 10 °C higher cutheat than measuring temperature. The test dose was approximate
46
47 to the anticipated D_e , and a 450 °C thermal wash was applied at the end of each
48
49 measurement cycle. SAR-ITL measured at 235 and 255 °C have been shown to give
50
51 reliable results. For MAR-TL, we did not observed any sensitivity change after the
52
53 initial thermal resetting. Results from both SAR-ITL and MAR-TL demonstrated
54
55
56
57
58
59
60
61
62
63
64
65

1 differences between the thermal histories of the samples. The D_e values from SAR-ITL
2
3 and MAR-TL overlapped after a 40-50 °C. SAR-ITL and MAR-TL are appropriate for
4
5
6 thermochronological studies.
7
8
9

10 11 **7. Acknowledgement**

12
13
14 This study was supported by the grants to SHL from the RGC of the Hong Kong SAR,
15
16
17 China (Project nos. 7028/08P, 7033/12P, 17303014). Sebastian Huot is grateful for
18
19
20 English editing and comments.
21
22
23
24
25
26
27
28
29
30
31
32
33
34
35
36
37
38
39
40
41
42
43
44
45
46
47
48
49
50
51
52
53
54
55
56
57
58
59
60
61
62
63
64
65

Reference:

- 1
2
3 Aitken, M.J., 1985. Thermoluminescence Dating. Academic Press Inc, London.
4
5
6 Aitken, M.J., Tite, M.S. and Reid, J., 1964. Thermoluminescent dating of ancient ceramics. *Nature* 202, 1032-1033.
7
8
9 Buylaert, J.P., Murray, A.S., Huot, S., Vriend, M.G.A., Vandenberghe, D. and De Corte, F., 2006. A comparison of quartz OSL and isothermal TL
10 measurements on Chinese loess. *Radiation protection dosimetry*, 119(1-4), 474-478.
11
12
13 Chen, R., and McKeever, S.W., 1997. Theory of thermoluminescence and related phenomena. Singapore: World Scientific.
14
15
16 Choi, J.H., Murray, A.S., Cheong, C.S., Hong, D.G. and Chang, H.W., 2006. Estimation of equivalent dose using quartz isothermal TL and the SAR
17 procedure. *Quaternary Geochronology*, 1(2), 101-108.
18
19
20 Dodson, M.H., 1973. Closure temperature in cooling geochronological and petrological systems. *Contributions to Mineralogy and Petrology* 40(3),
21 259-274.
22
23
24 Duller, G. A. T., 2003. Distinguishing quartz and feldspar in single grain luminescence measurements. *Radiation Measurements*, 37(2), 161-165.
25
26
27 Han, Z.Y., Li, S.H. and Tso, M.Y.W., 1997. Age dependence of luminescence signals from granitic and mylonitic quartz. *Quaternary Science Reviews*,
28 16(3), 427-430.
29
30
31 Herman, F., Rhodes, E.J., Braun, J. and Heiniger, L., 2010. Uniform erosion rates and relief amplitude during glacial cycles in the Southern Alps of
32 New Zealand, as revealed from OSL-thermochronology. *Earth and Planetary Science Letters*, 297(1), 183-189.
33
34
35
36 Hornyak, W.F., Chen, R. and Franklin, A., 1992. Thermoluminescence characteristics of the 375 C electron trap in quartz. *Physical Review B*, 46(13),
37 8036-8049.
38
39
40
41
42
43
44
45
46
47
48
49
50
51
52
53
54
55
56
57
58
59
60
61
62
63
64
65
- Li, B. and Li, S.H., 2011. Luminescence dating of K-feldspar from sediments: a protocol without anomalous fading correction. *Quaternary Geochronology* 6(5), 468-479.
- Li, B. and Li, S.H., 2012. Determining the cooling age using luminescence-thermochronology. *Tectonophysics*, 580, 242-248.
- Li, S.H., Sun, J.M. and Zhao, H., 2002. Optical dating of dune sands in the northeastern deserts of China. *Palaeogeography, Palaeoclimatology, Palaeoecology*, 181(4), 419-429.
- Jain, M., Bøtter-Jensen, L., Murray, A.S., Denby, P.M., Tsukamoto, S. and Gibling, M.R., 2005. Revisiting TL: Dose measurement beyond the OSL range using SAR. *Ancient TL* 23, 9-24.
- Johnson, N.M., 1966. Geothermometry from the thermoluminescence of contact-metamorphosed limestone. *Journal of Geology*. 74, 607-619.
- Mejdahl, V. and Bøtter-Jensen, L., 1994. Luminescence dating of archaeological materials using a new technique based on single aliquot

1 measurements. *Quaternary Science Reviews*, 13(5), 551-554.

2
3 Murray, A.S. and Wintle, A.G., 2000b. Application of the single-aliquot regenerative-dose protocol to the 375 C quartz TL signal. *Radiation*
4 *Measurements*, 32(5), 579-583.

5
6
7 Murray, A.S. and Wintle, A.G., 2000a. Luminescence dating of quartz using an improved single-aliquot regenerative-dose protocol. *Radiation*
8 *measurements*, 32(1), 57-73.

9
10
11 Murray, A.S. and Wintle, A.G., 2003. The single aliquot regenerative dose protocol: potential for improvements in reliability. *Radiation Measurements*,
12 37(4), 377-381.

13
14
15 Nambu, M., Mikami, K., Tsuchiya, N. and Nakatsuka, K., 1996. Thermoluminescence of quartz in the borehole cores from the Minase Geothermal
16 Area, Akita Prefecture, Japan. *Journal-Geothermal research society of Japan*, 18, 39-49.

17
18
19 Prescott, J.R., Huntley, D.J. and Hutton, J.T., 1993. Estimation of equivalent dose in thermoluminescence dating—the Australian slide method.
20 *Ancient TL*, 11(1), 1-5.

21
22
23 Prokein, J. and Wagner, G.A., 1994. Analysis of thermoluminescent glow peaks in quartz derived from the KTB-drill hole. *Radiation measurements*,
24 23(1), 85-94.

25
26
27 Tribolo, C. and Mercier, N., 2012. Towards a SAR-ITL protocol for the equivalent dose estimate of burnt quartzites. *Ancient TL*, 30, 17-25.

28
29
30 Tsuchiya, N., Suzuki, T. and Nakatsuka, K., 2000. Thermoluminescence as a new research tool for the evaluation of geothermal activity of the
31 Kakkonda geothermal system, northeast Japan. *Geothermics*, 29(1), 27-50.

Figure caption:

Fig. 1: Typical ITL and TL signal (from sample FG-A).

Fig. 2: A, B and C: ITL signals at 235 °C with different preheat conditions. The primary y-axis shows the ITL counts and the secondary y-axis shows the ratio between natural and regenerative signals. D: D_e plot of SAR-ITL at 235 °C against test dose. The dashed line shows the mean of D_e values by using test doses of 145 and 250 Gy, and the yellow shaded region shows the standard deviation. E: D_e plot of SAR-ITL at 235 °C against cycle clear-up temperatures.

Fig. 3: SAR-ITL natural signals at heating temperatures of 215, 235, 255, 275, 295 °C.

Fig. 4: SAR-ITL and MAR-TL protocol.

Fig. 5: A comparison between additive and regenerative dose growth curve of TL signal. The TL counts were normalized by 140 Gy second glow TL signals.

Fig. 6: $D_e(T)$ plot of MAR-TL results by 215, 235, 255 °C cutheat. The D_e values were calculated by interpolating the mean natural TL signals of six aliquots onto a regenerated growth curve, from TL signals of six aliquots.

1
2
3
4
5
6
7
8
9
10
11
12
13
14
15
16
17
18
19
20
21
22
23
24
25
26
27
28
29
30
31
32
33
34
35
36
37
38
39
40
41
42
43
44
45
46
47
48
49
50
51
52
53
54
55
56
57
58
59
60
61
62
63
64
65

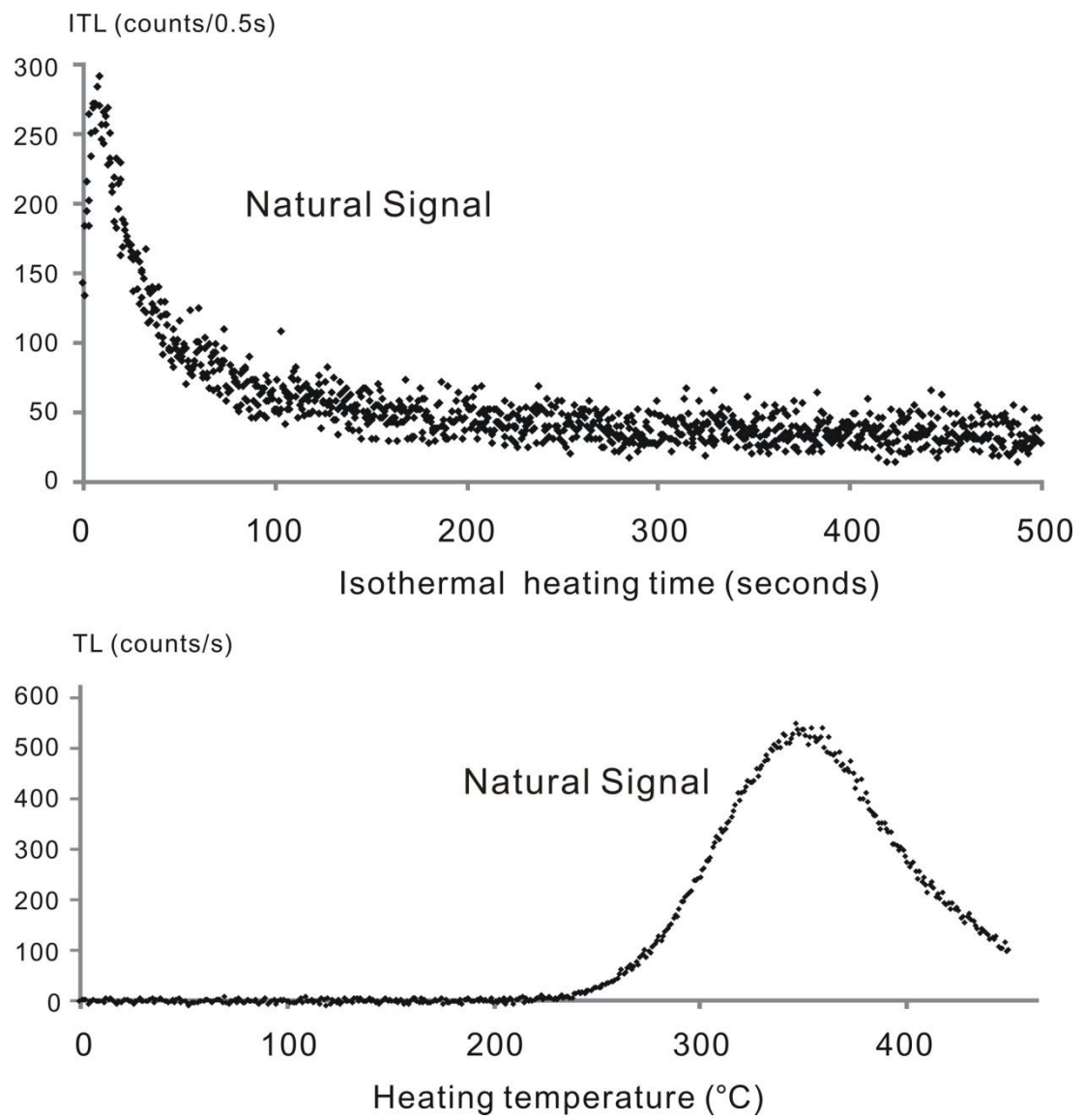


Fig. 1

1
2
3
4
5
6
7
8
9
10
11
12
13
14
15
16
17
18
19
20
21
22
23
24
25
26
27
28
29
30
31
32
33
34
35
36
37
38
39
40
41
42
43
44
45
46
47
48
49
50
51
52
53
54
55
56
57
58
59
60
61
62
63
64
65

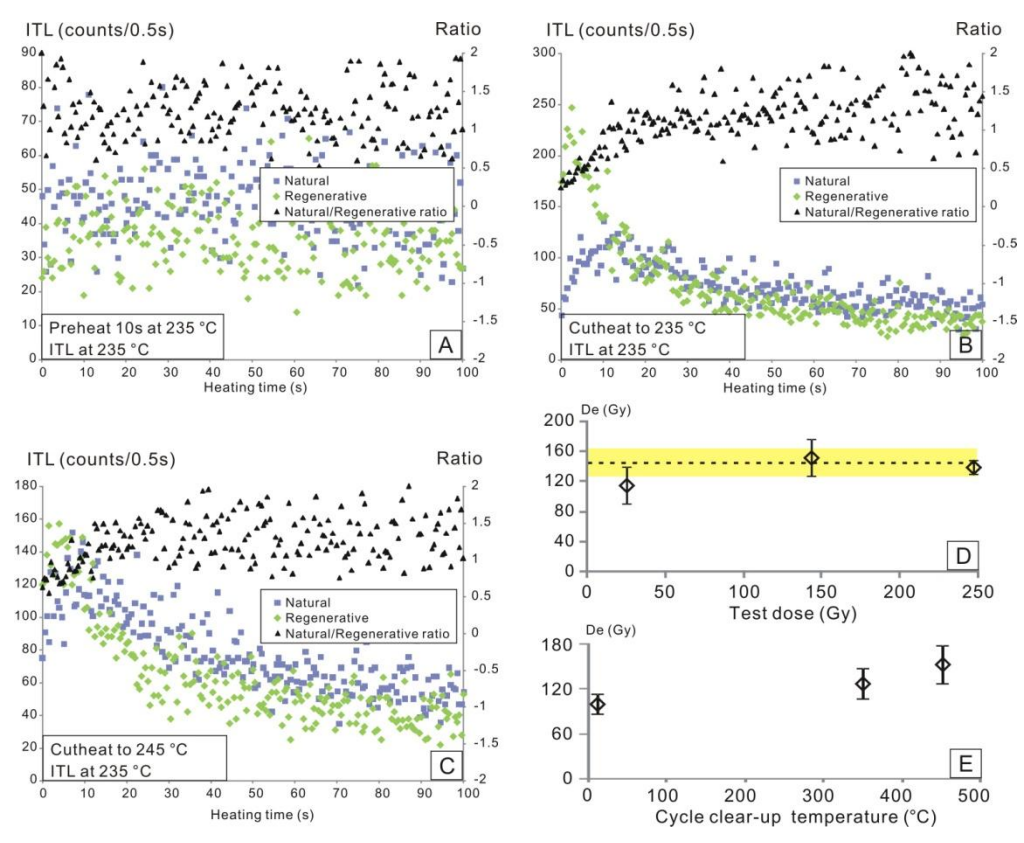


Fig. 2

1
2
3
4
5
6
7
8
9
10
11
12
13
14
15
16
17
18
19
20
21
22
23
24
25
26
27
28
29
30
31
32
33
34
35
36
37
38
39
40
41
42
43
44
45
46
47
48
49
50
51
52
53
54
55
56
57
58
59
60
61
62
63
64
65

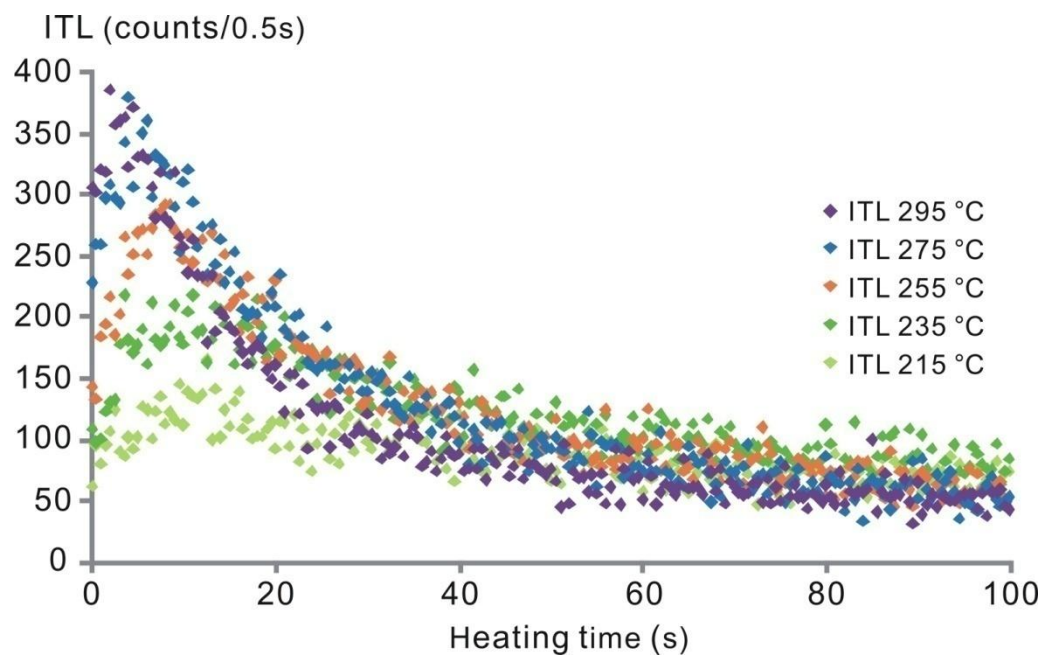
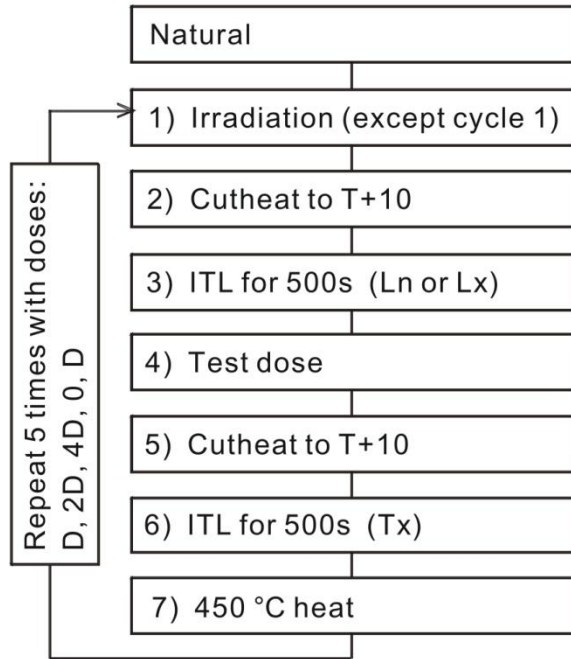


Fig. 3

A) SAR-ITL protocol



B) MAR-TL protocol

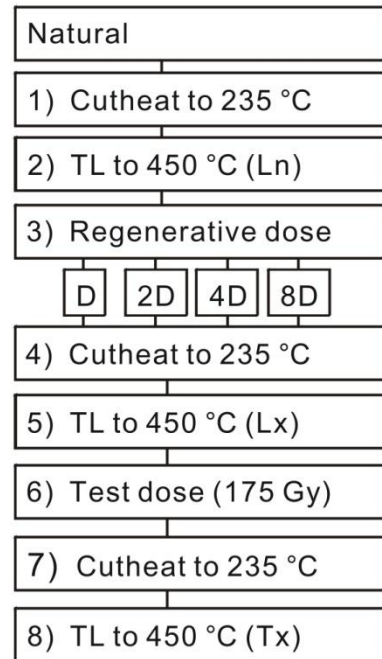


Fig. 4

1
2
3
4
5
6
7
8
9
10
11
12
13
14
15
16
17
18
19
20
21
22
23
24
25
26
27
28
29
30
31
32
33
34
35
36
37
38
39
40
41
42
43
44
45
46
47
48
49
50
51
52
53
54
55
56
57
58
59
60
61
62
63
64
65

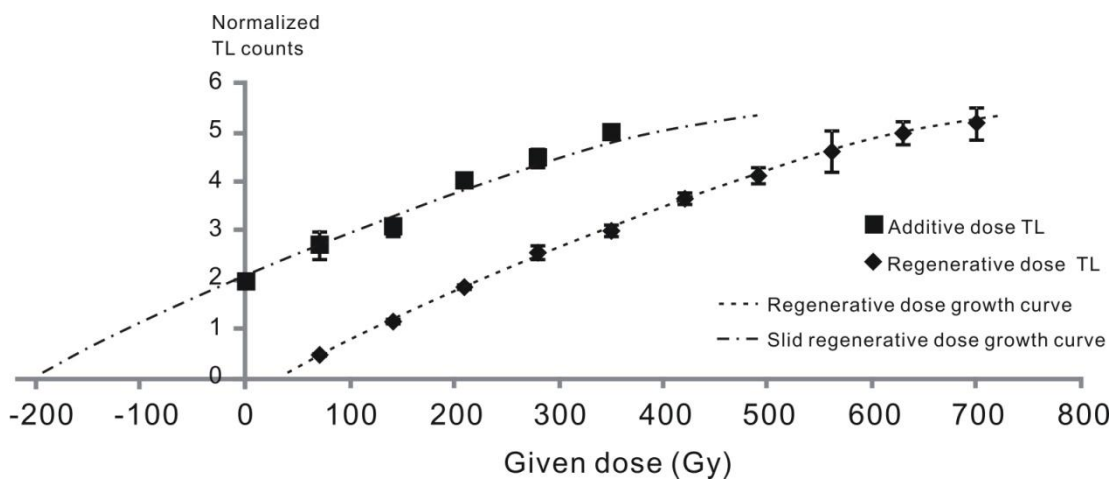


Fig. 5

1
2
3
4
5
6
7
8
9
10
11
12
13
14
15
16
17
18
19
20
21
22
23
24
25
26
27
28
29
30
31
32
33
34
35
36
37
38
39
40
41
42
43
44
45
46
47
48
49
50
51
52
53
54
55
56
57
58
59
60
61
62
63
64
65

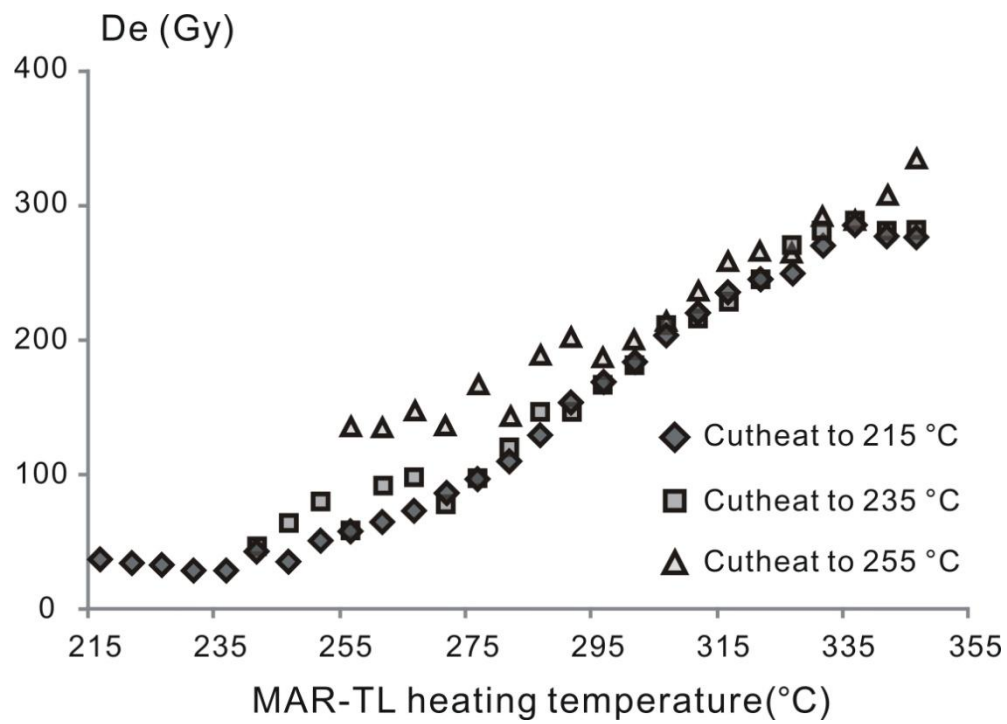


Fig. 6

Table 1 The results of SAR-ITL and MAR-TL

| Sample | De of SAR-ITL (Gy) | | De of MAR-TL (Gy) | | | | | | | | |
|--------|--------------------|-------------|-------------------|-------------|-------------|-------------|-------------|-------------|-------------|--------------|--------------|
| | At 235 °C | At 255 °C | At 250 °C | At 260 °C | At 270 °C | At 280 °C | At 290 °C | At 300 °C | At 310 °C | At 320 °C | At 330 °C |
| FG-A | 153.2 ±25.3 | 258.4 ±19.6 | 49.2 ±11.4 | 66.4 ±13.7 | 93.0 ±12.0 | 127.4 ±14.7 | 166.6 ±14.1 | 220.5 ±14.6 | 273.7 ±14.7 | 338.7 ±23.3 | 387.7 ±39.1 |
| FG-B | 200.6 ±19.2 | 350.8 ±30.1 | 76.9 ±18.0 | 102.6 ±20.1 | 146.5 ±27.2 | 204.1 ±32.9 | 271.1 ±41.0 | 337.9 ±47.5 | 394.5 ±51.0 | 451.3 ±60.7 | 476.1 ±68.0 |
| FG-C | 48.9 ±6.9 | 200.7 ±28.2 | 63.3 ±19.5 | 79.4 ±21.5 | 104.1 ±27.6 | 124.6 ±34.5 | 176.8 ±52.5 | 230.1 ±69.1 | 305.2 ±84.5 | 355.4 ±104.5 | 413.7 ±116.3 |